Available online at www.sciencedirect.com
ScienceDirect
Journal of Photochemistry and Photobiology A: Chemistry 183 (2006) 261–266
Journal of Photochemistry and Photobiology A:Chemistry
www.elsevier.com/locate/jphotochem

Higher-order multiphoton imaging by femtosecond near-infrared laser microscope system

Hirohisa Matsuda [a,1], Syoji Ito [a], Yutaka Nagasawa [a], Tsuyoshi Asahi [b], Hiroshi Masuhara [b], Seiya Kobatake [c], Masahiro Irie [d], Hiroshi Miyasaka [a,*]

[a] *Division of Frontier Materials Science, Graduate School of Engineering Science, Center for Quantum Science and Technology under Extreme Conditions, Osaka University, Toyonaka, Osaka 560-8531, Japan*
[b] *Department of Applied Physics, Graduate School of Engineering, Osaka University, Suita, Osaka 565-0871, Japan*
[c] *Department of Applied Chemistry, Graduate School of Engineering, Osaka City University, Sumiyoshi, Osaka 558-8585, Japan*
[d] *Department of Chemistry and Biochemistry, Graduate School of Engineering, Kyusyu University, Fukuoka 812-8585, Japan.*

Available online 28 April 2006

Abstract

Near-infrared (NIR) femtosecond laser microscope with Cr:Forsterite laser at ca. 1.26 μm output wavelength was constructed and applied to two-, three- and four-photon imaging of gold nanoparticle and some organic micro crystals. The ultrafast pulse duration of 35 fs after passing through the objectives easily induced higher-order multiphoton absorption. The size of the laser focal spot and the resolution along the optical axis were discussed by comparing the present higher-order multiphoton imaging and two-photon induced processes.

Keywords: Chromium:forsterite laser; Near-infrared femtosecond microscopy; Three-photon imaging; Four-photon imaging

1. Introduction

The application of optical microscopic techniques into mesoscopic systems has been providing detailed information on properties and reactions in these systems, e.g. microreactor, droplet, micrometer-sized organic crystal, and dynamics of single molecular and single particle [1,2] and the introduction of the pulsed laser light source in these microscopes have been enabling the direct information of dynamic behaviors depending on the molecular environment, crystal shape and so on [3]. Microscopy with femtosecond lasers is a typical tool to pursue the dynamics with sub-picosecond temporal resolution and sub-micrometer spatial resolution. Femtosecond lasers can easily induce the multiphoton absorption process [4] because of their high photon density. An application of this multiphoton excitation to optical microscopy started with the proposal of two-photon laser scanning fluorescence microscopy by Denk et al. [5] and has been proved several advantages in the spatial resolution in addition to easy separation of excitation and emission light resulting in the enhanced signal-to-noise (S/N) ratio. This spatial selectivity of the multiphoton excitation is used not only for the imaging but also for microprocessing [6] and stereolithography [7].

Since the probability of multiphoton absorption process is a function of the peak intensity of the incident light, the application of laser pulse with shorter pulse duration is one of the general methods to spatially and temporally attain high photon density. Pulse duration under a microscope, however, is mainly limited by the dispersion of an objective and typically stays in several hundreds of femtosecond in the case that Ti:Sapphire laser around 800 nm is employed as a light source. On the other hand, application of near-infrared (NIR) laser with longer wavelength (>1 μm) output may lead to the realization of much shorter pulse duration under objectives due to less dependence on the wavelength of refractive index leading to the small dispersion in these wavelength regions. In addition, the application of the longer wavelength pulse has more advantages such as lower probability of light scattering resulting in deeper penetration into opaque medium and less photodegradation of samples [8–11].

* Corresponding author. Tel.: +81 6 6850 6241; fax: +81 6 6850 6244.
E-mail address: miyasaka@chem.es.osaka-u.ac.jp (H. Miyasaka).
[1] JSPS Research Fellow (PD).

1010-6030/$ – see front matter © 2006 Elsevier B.V. All rights reserved.
doi:10.1016/j.jphotochem.2006.04.014

From these viewpoints, we recently developed an NIR femtosecond optical microscope whose pulse duration at the sample position after 100× objective was 35 fs by using home-build Cr:Forsterite (Cr:F) laser [12,13] with the oscillation centered at 1.26 μm [14]. The short pulse duration of 35 fs enabled the detection of higher-order multiphoton fluorescence in organic crystals with lower photo-degradation threshold than inorganic semiconductors [15]. The excitation intensity dependence and the interferometric detection of the multiphoton fluorescence intensities of organic crystals as a function of the time interval between the two NIR laser pulses clearly showed that these fluorescence signals were due to simultaneous three- and four-photon absorption processes for perylene and anthracene micro crystals, respectively.

In the present paper, we have applied this microscope to the imaging through the multiphoton processes; simultaneous two-photon reaction in a photochromic diarylethene crystal [16], second-harmonic generation (SHG) of aggregated gold nanoparticle, and three- and four-photon fluorescence of organic micro crystals. By comparing the three-photon fluorescence imaging [17–21] with the present results, we will discuss the higher-order multiphoton imaging by the NIR femtosecond laser microscope system.

2. Experimental

Details of the home-built femtosecond Cr:F laser was described elsewhere [12,13]. In brief, the cavity of the Cr:F laser consisted of six mirror, 19 mm Cr:F crystal as the laser medium, SF6 Brewster prism pair and a Bragg cell for cavity dumping (Fig. 1(a)). The output energy of the Cr:F laser around 1.26 μm was 10 nJ at 625 kHz repetition rate.

The pulse was introduced to an optical microscope through a chirp–compensation prism pair. The pulse width at the sample plane was 35 fs FWHM with a 100× objective (Mplan 100× IR, Olympus, NA = 0.95) on the basis of the interferometric second-order harmonic (SHG) autocorrelation with BBO crystal [14]. The emission from the sample was detected after passing through a pinhole with diameter of 100 μm by an avalanche photodiode (SPCM-AQR-14, Perkin-Elmer) connected to a photon counter (SR400, Stanford Research Systems) or a fiber-coupled spectrometer (SD2000, Ocean Optics) without the pinhole. Two-photon fluorescence autocorrelation was measured by an avalanche photodiode (C5460-1, Hamamatsu) with a lock-in amplifier (model 5210, EG & G Instruments). The relative position between the sample and the focus was controlled by a stepping motor stage (BIOS-405T, SIGMA

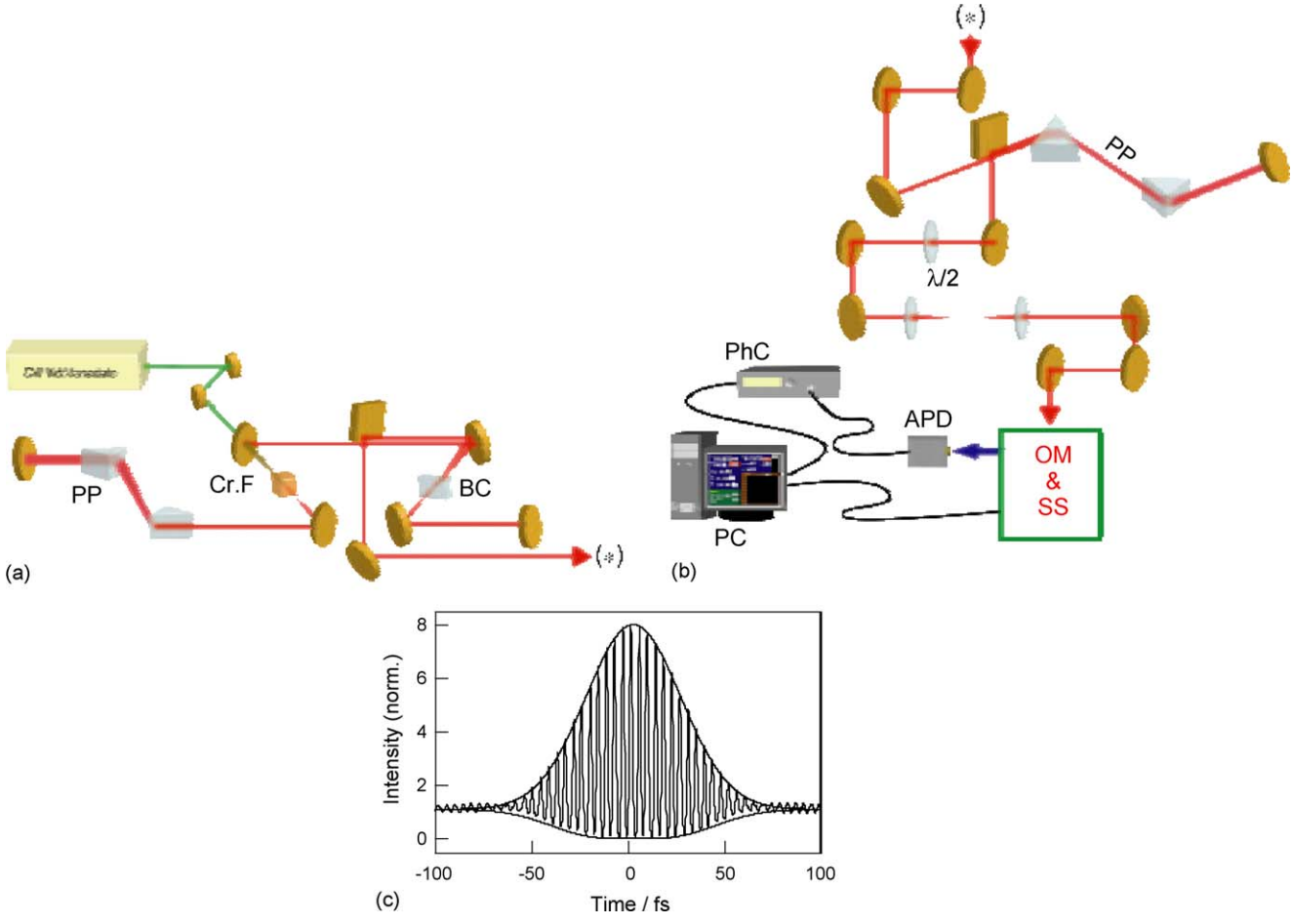

Fig. 1. (a) Block diagram of the femtosecond Cr:F laser and (b) optical system of the NIR laser microscope: PP, prism pair; Cr:F, chromium:forsterite crystal; BC, Brag cell; λ/2, halfwave plate; PhC, photon counter; APD, avalanche photodiode; OM, optical microscope; SS, scanning stage. (c) Interferometric two-photon fluorescence autocorrelation trace and envelope curve assuming a chirp-free Gaussian pulse with 35 fs FWHM.

KOKI) in horizontal plane and a piezo stage (SFS-OBL-1, SIGMA KOKI) along optical axis, respectively (Fig. 1(b)). Movements of these stages and data-acquisition of the photon counter were synchronized by home-made PC software. Transmittance images were measured by using a color CCD camera (HCC-600, Flovel) and a high-sensitivity CCD camera (Cascade II 512 B, Roper Scientific Inc.). Fig. 1(c) shows the interferometric two-photon fluorescence autocorrelation trace of Nile Blue (Exciton) dissolved in ethylene glycol (Wako) at the sample position of the microscope. The solid line for the envelope is the curve calculated on the assumption that the pulse shape and the pulse width (FWHM) are Gaussian and 35 fs, respectively.

1,2-Bis(2-methoxy-4-methyl-5-phenyl-3-thienyl)perfluorocyclopentene, a photochromic diarylethene derivative, was synthesized, purified, and crystallized [22]. The closed-ring isomer has an absorption band around 655 nm, while the open-form isomer is transparent in the visible region.

Perylene (sublimation, Aldrich) and anthracene (zone-refined, Aldrich) were purified by recrystallization from ethanol. Microcrystals of anthracene and perylene were obtained by spin coating of their tetrahydrofuran (infinity-pure, Wako) solution on cover glass. Gold nanoparticle with diameter of 100 nm (EMGC.100, BB International) was used as received. The aggregated nanoparticle was prepared by evaporation of the dispersion solution. All measurements were performed at $(22 \pm 1)\,^{\circ}C$.

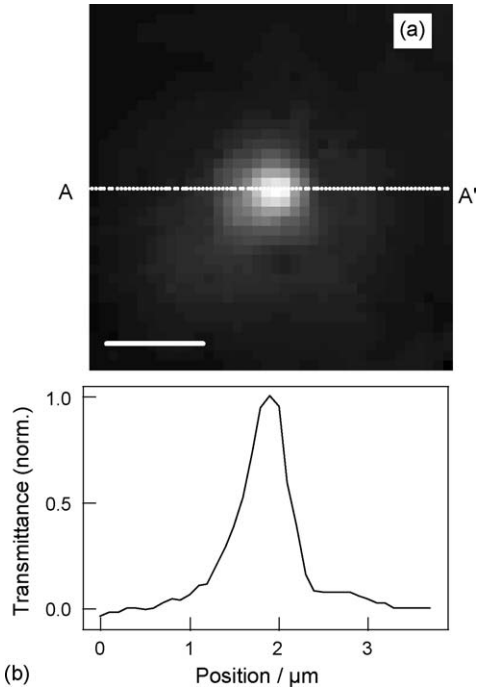

Fig. 2. (a) Optical transmittance image of diarylethene crystal after irradiation of femtosecond NIR pulse with power of 320 pJ/pulse in 3 min. The center of crystal was converted from the colored (closed-ring) isomer to the colorless (open-ring) isomer looks white and the other part stays dark. Scale bar: 1 μm. (b) Image line profile of (a) along a line from A to A′. FWHM of the profile is 550 nm.

3. Results and discussion

In order to experimentally determine the focal spot size of the NIR laser under the microscope, we utilized the photochromic reaction of a diarylethene crystal, 1,2-bis(2-methoxy-4-methyl-5-phenyl-3-thienyl)perfluorocyclopentene (PCI). First, we prepared the colored crystal in the following manner. Continuum UV light irradiation (4.5 mW/cm^2) in 10 min of the colorless crystal of PCI (open-form isomer) induces a photochromic cyclization reaction resulting in the production of the crystal where surface area was converted into the colored closed-ring isomer with an absorption band around 655 nm.

Because the two-photon energy of the fundamental light at 1.26 μm corresponds to the light at 630 nm, the excitation of the close-ring isomer can be attained by the two-photon absorption

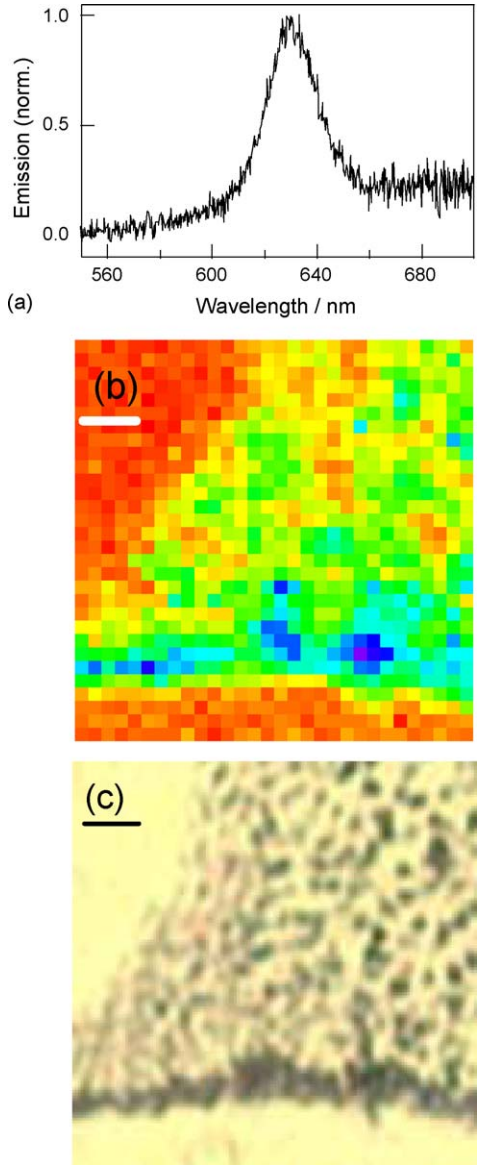

Fig. 3. (a) Emission spectrum and (b) two-photon image of the aggregated gold nanoparticles, obtained with the excitation of the femtosecond NIR laser pulse centered at 1.26 μm. Excitation power was 250 pJ/pulse and scanning step was 500 nm. (c) Transmission image. Scale bars in (b and c) correspond to 2 μm.

process of the Cr:F laser. Hence, the information on the focal spot size can be obtained from the area where the cycloreversion reaction takes place by NIR laser pulses.

Fig. 2 shows an optical transmittance image of the diarylethene crystal after the irradiation of femtosecond NIR pulse with the output energy of 320 pJ/pulse (625 kHz) for 3 min. The center of crystal was converted from the colored form to the colorless isomer (white color in the figure), while unirradiated area stays dark. After the NIR laser pulse irradiation, it was confirmed that the white area was converted again into the colored closed-ring isomer by the irradiation of the UV light. Hence, the white area can be safely ascribed to the bleaching due to the photochromic reaction via two-photon excitation. Because the present diarylethene derivative does not undergo reactions between the colored- and colorless isomers in the electronic ground state, the size of white spot in Fig. 2(a) corresponds to the reaction area due to the two-photon induced isomerization.

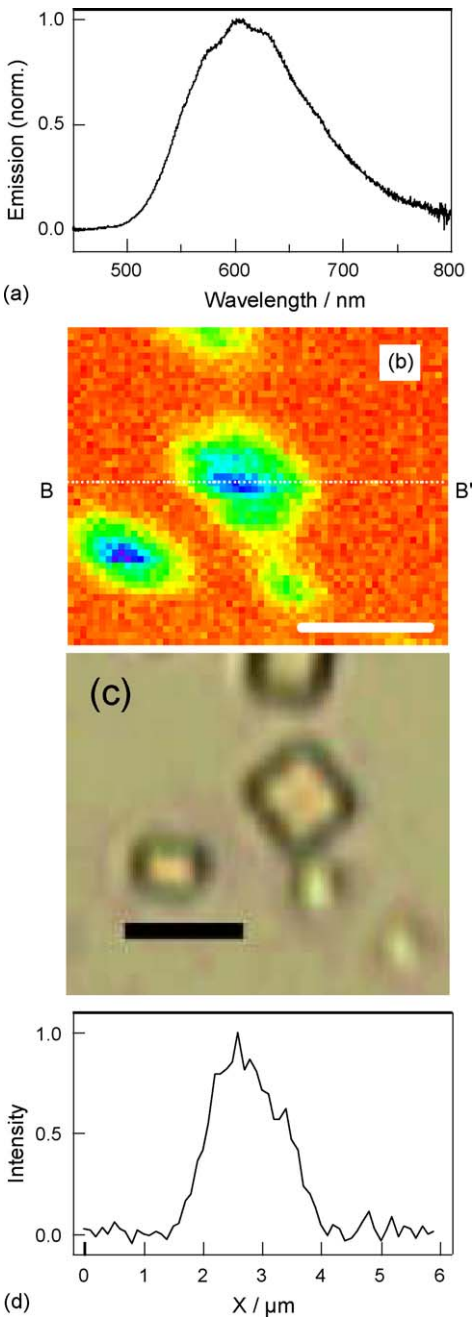

Fig. 4. (a) Emission spectrum and (b) three-photon fluorescence image of perylene microcrystal, obtained with the excitation of the femtosecond NIR laser pulse centered at 1.26 μm. Excitation power was 70 pJ/pulse and scanning step was 100 nm. (c) Transmittance image of perylene crystal. (d) Cross-section along B–B′ line in (b). Scale bars in (b and c) correspond to 2 μm.

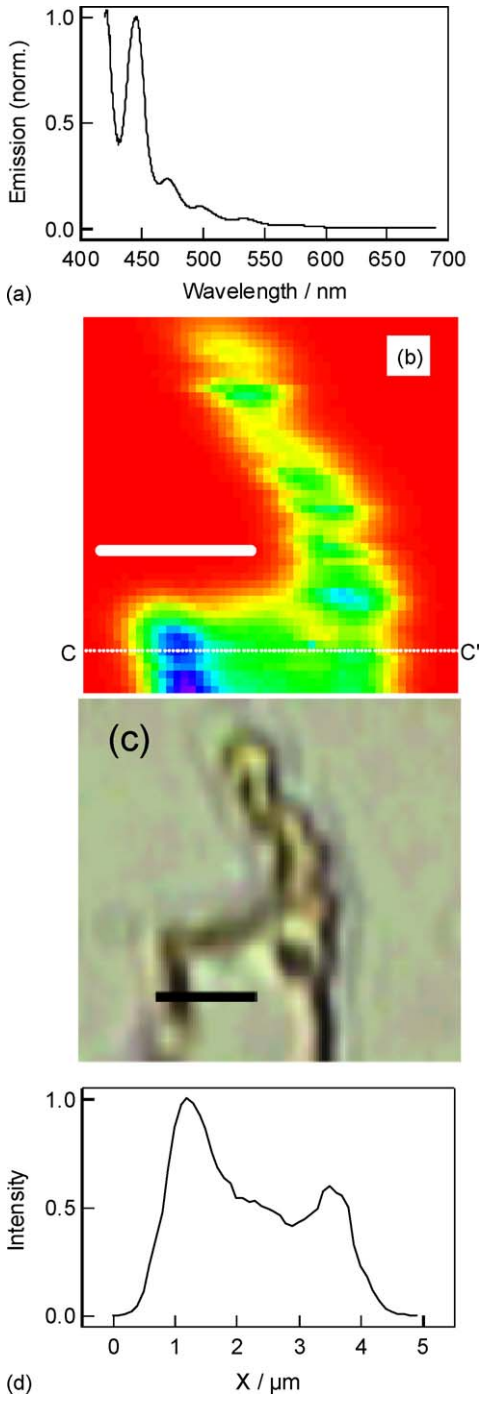

Fig. 5. (a) Emission spectrum, (b) four-photon fluorescence image of anthracene crystal with excitation power of 400 pJ/pulse and a scanning step of 100 nm, and (c) transmittance of the same area with (b). (d) Cross-section along C–C′ line in (b). Scale bar: 2 μm.

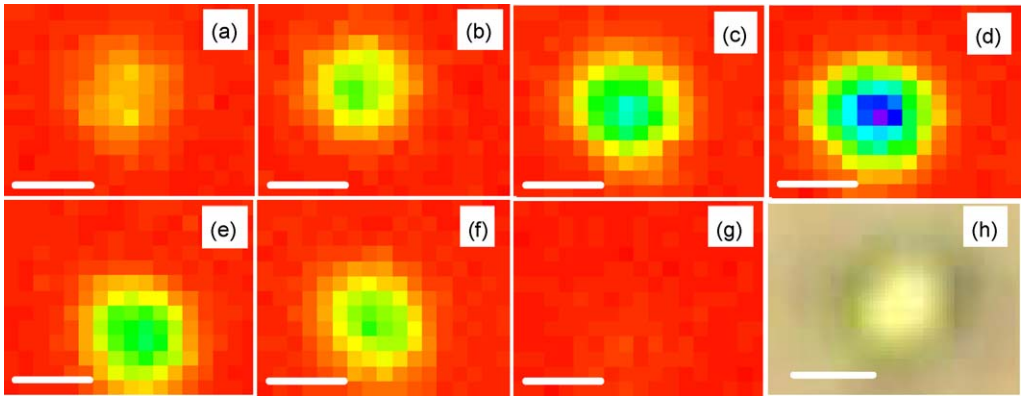

Fig. 6. Set of four-photon fluorescence optical section of an anthracene crystal. The sections are separated by 400 nm, where (a to g) are closest to glass substrate and objective, respectively. (h) Transmittance image of scanned area. Scale bar: 500 nm.

A transmittance profile along the line from A to A′ in Fig. 2(a) is shown in Fig. 2(b). The FWHM of Fig. 2(b) is ca. 550 nm. This value is very close to or slightly larger than the FWHM of two-photon induced accessible size based on diffraction limit (490 nm) under the condition that the objective with NA = 0.95 and the irradiation at 1.26 μm are employed, indicating that the above results indicated optical setup of the NIR laser microscope provides the sub-micrometer resolution.

Fig. 3 shows the emission spectrum (a), emission image (b), and transmission image (c) of the aggregated gold nanoparticles. In Fig. 3(a and b), the excitation laser power was 250 pJ/pulse. The emission spectrum in Fig. 3(a) almost agrees with the laser output spectrum whose abscissa is converted to twice the energy. The irradiation of gold nanoparticles by intense laser light results in the second-harmonic generation through the interaction between the surface plasmon and the light [23]. Hence, the present emission is mainly ascribed to the second-harmonic of the incident laser output. Fig. 3(c) shows the high-density area of the aggregated gold nanoparticle in the bottom with belt shape and low-density area in the upper. Fig. 3(b) well reproduces this difference in particle density shown in Fig. 3(c).

Fig. 4(a) shows the emission spectrum of perylene microcrystal excited with the NIR femtosecond laser pulse under the microscope. Broad emission spectrum with a maximum at 605 nm is ascribed to the self-trapped exciton in the α-typed perylene crystal [24]. The spectrum clearly shows that the irradiation of the femtosecond NIR laser pulse results in the production of the excited singlet state in these crystals. Excitation intensity dependence and interferometric fluorescence detection revealed that the simultaneous three-photon absorption of the incident light at 1.26 μm is responsible for the excitation of the perylene molecule [14].

Fig. 4(b and c) shows the three-photon fluorescence and optical transmission images of perylene microcrystals, respectively. In Fig. 4(b), the excitation power was 70 pJ/pulse. Fig. 4(d) shows the cross-section along B–B′ line in Fig. 4(b), and the perylene crystal sizes ca. 1.8 and 2.5 μm in transmission and three-photon fluorescence image, respectively. The size of fluorescence image was lager than that of transmission. The difference of the sizes in transmittance and fluorescence image is consistent by taking accessible size of three-photon reaction (400 nm, FWHM) based on diffraction limit into consideration.

Fig. 5(a) shows the emission spectrum of anthracene microcrystal excited with the NIR femtosecond laser pulse under the microscope. Wavelength region <420 nm was not detected because of the low transmittance of the dichroic mirror. The emission with several vibronic structures of the anthracene crystal is safely ascribed to the fluorescence due to the free-exciton in the crystalline state [25]. Excitation intensity dependence and interferometric autocorrelation detection of the fluorescence intensity revealed that simultaneous four-photon absorption process was responsible for the fluorescence [14]. Fig. 5(b and c) shows the fluorescence and the optical transmission images of anthracene microcrystal, respectively. In Fig. 5(b), the excitation power was 400 pJ/pulse. The characteristic structure of the anthracene microcrystal in Fig. 5(c) was well reproduced in Fig. 5(b). Fig. 5(d) shows cross-section along C–C′ line in Fig. 5(b). The width of the microcrystal along this line is ca. 3.7 μm in optical transmission, while it is ca. 4.0 μm in four-photon fluorescence image. The difference of crystal size between two images is smaller than that in the three-photon imaging. This can reflect improvement of the spatial resolution due to higher-order multiphoton fluorescence. After experiment, no photodamage of sample in both three- and four-photon imaging was recognized, though the three- and four-photon absorption cross-section is very small [14].

Multiphoton imaging has an intrinsic advantage of three-dimensional resolution. Fig. 6 shows a set of horizontal four-photon intensity mapping of an anthracene crystal. Each frame in Fig. 6(a–g) was measured by every 400 nm in optical axis. Fig. 6(g) is closest to the objective. The excitation laser was 200 pJ/pulse. Each figure clearly shows the capability of the four-photon fluorescence imaging along optical axis in sub micrometer scale.

4. Summary

The present NIR laser microscope was applied to the imaging of multiphoton fluorescence up to four-photon absorption without any photodamage, despite of small cross-section of higher-order multiphoton absorption. To our knowledge, this is

the first imaging utilizing four-photon fluorescence of organic crystals. In addition to the temporal resolution of 35 fs and higher multiphoton imaging, it is worth mentioning that the excited states attained by two-, three- and four-photon excitation of the present Cr:F laser corresponds to 630, 420 and 315 nm, respectively. These modes of excitation can cover the absorption band from visible to ultraviolet. Compared to the multiphoton laser microscope with Ti:Sapphire laser oscillating around 800 nm, the present femtosecond Cr:F laser microscope has wider selectivity of the fluorescence compounds. This may lead to the utilization in the multicolor fluorescence imaging without introduction of multiple dichroic mirrors and multiple blocking filters. We are now studying these multicolor imaging, results of which will be published soon.

Acknowledgements

This work was partly supported by Grant-in-Aids for Scientific Research on Priority Areas "Molecular Nano Dynamics" (432) and (No. 16350012) from the Ministry of Education, Culture, Sports, Science, and Technology (MEXT) of the Japanese Government.

References

[1] (a) H. Masuhara, F.C. De Schryver, N. Kitamura, N. Tamai (Eds.), Microchemisiry: Spectroscopy and Chemistry in Small Domains, North-Holland, Amsterdam, 1994.
(b) H. Masuhara, H. Nakanishi, K. Sasaki (Eds.), Single Organic Nanoparticle, Springer, Berline, 2003.
[2] (a) T. Basché, W.E. Moerner, M. Orrit, U.P. Wild (Eds.), Single Molecule Optical Detection, Imaging and Spectroscopy, Verlag-Chemie, Munich, 1997.
(b) R. Rigler, M. Orrit, T. Basché (Eds.), Single Molecule Spectroscopy, Springer, Berlin, 2002.
[3] H. Matsune, T. Asahi, H. Masuhara, H. Kasai, H. Nakanishi, Mater. Res. Soc. Symp. Proc. 846 (2005) DD10.8.
[4] M. Göppert-Mayrer, Ann. Phys. 9 (1931) 273.
[5] W. Denk, J.H. Strickler, W.W. Webb, Science 248 (1990) 73.
[6] B.H. Cumpston, S.P. Ananthavel, S. Barlow, D.L. Dyer, J.E. Ehrlich, L.L. Erskine, A.A. Heikal, S.M. Kuebler, I.-Y.S. Lee, D. McCord-Maughon, J. Qin, H. Röckel, M. Rumi, X.-Li. Wu, S.R. Marder, J.W. Perry, Nature 398 (1999) 51.
[7] S. Maruo, O. Nakamura, S. Kawata, Opt. Lett. 22 (1997) 132.
[8] R.R. Anderson, J.A. Parrish, J. Invest. Dermatol. 77 (1981) 77.
[9] S.W. Chu, I.-H. Chen, T.M. Liu, P.C. Cheng, C.-K. Sun, B.-L. Lin, Opt. Lett. 26 (2001) 1909.
[10] E. Abraham, E. Bordenave, N. Tsurumachi, G. Jonusauskas, J. Oberlé, C. Rullière, A. Mito, Opt. Lett. 25 (2000) 929.
[11] I.-H. Chen, S.-W. Chu, C.-K. Sun, P.-C. Cheng, B.-L. Lin, Opt. Quant. Electron. 34 (2002) 1251.
[12] Y. Nagasawa, Y. Ando, A. Watanabe, T. Okada, Appl. Phys. B 70 (2000) S33.
[13] H. Matsuda, Y. Nagasawa, H. Miyasaka, T. Okada, J. Photo. Photo. A 156 (2003) 69.
[14] H. Matsuda, Y. Fujimoto, S. Ito, Y. Nagasawa, H. Miyasaka, T. Asahi, H. Masuhara, J. Phys. Chem. B 110 (2006) 1091.
[15] Just before the publication of Ref. [14], the four-photon microscopy with Cr:F laser with pulse width of 140 fs was applied to the detection of luminescence of GaN. S.-W. Chu, M.-C. Chan, S.-P Tai, S. Keller, S.P. DenBaars, C.-K. Sun, Opt. Lett. 30 (2005) 2463.
[16] M. Irie, Chem. Rev. 100 (2000) 1685.
[17] C. Xu, W. Zipfel, J.B. Shear, R.M. Williams, W.W. Webb, Proc. Natl. Acad. Sci. 93 (1996) 10763.
[18] S.W. Hell, K. Bahlmann, M. Schrader, A. Soini, H. Malak, I. Gryczynski, J.R. Lakowicz, J. Biomed. Opt. 1 (1996) 71.
[19] S. Maiti, J.B. Shear, R.M. Williams, W.R. Zipfel, W.W. Webb, Science 275 (1997) 530.
[20] M. Gu, Opt. Lett. 21 (1996) 988.
[21] C.J.R. Sheppard, Bioimaging 4 (1996) 124.
[22] S. Kobatake, Y. Matsumoto, M. Irie, Angew. Chem. Int. Ed. 44 (2005) 2148.
[23] H. Wang, E.C.Y. Yan, E. Borguet, K.B. Eisenthal, Chem. Phys. Lett. 259 (1996) 15.
[24] H. Nishimura, T. Yamaoka, K. Mizuno, M. Iemura, A. Matsui, J. Phys. Soc. Jpn. 53 (1984) 3999.
[25] H. Nishimura, T. Yamaoka, K. Hattori, A. Matsui, K. Mizuno, J. Phys. Soc. Jpn. 54 (1985) 4370.